Biotechnological Journal of Environmental Microorganisms (BJEM)

Biotechnological Journal of Environmental Microorganisms(BJEM) 2(5) 2023 244-252

Characterization of Hydrothermally Grown Pure and Graphene added Samarium Oxide Nano-Structures as a Potential Antimicrobial agent

A. Bagheri Khatibani*[1], Somayeh Saadat Niavol[2], Samaneh Rasouli Jamnani[3], Hosein Milani Moghaddam[4]

[1] Nano Research Lab, Lahijan Branch, Islamic Azad University, P.O. Box 1616, Lahijan, Iran
[2] Department of Solid State Physics, University of Mazandaran, 4741695447 Babolsar, Iran
[3] Department of Solid State Physics, University of Mazandaran, 4741695447 Babolsar, Iran
[4] Department of Solid State Physics, University of Mazandaran, 4741695447 Babolsar, Iran
Received: 14 April 2023/ Revised: 28 April 2023/ Accepted: 07 May 2023

Abstract

Seductive and impressive applications of samarium oxide based materials in semiconductor science, created an interest to synthesize and study their physical properties. Therefore, after preparing pure samarium oxide and graphene/samarium oxide powders through hydrothermal technique; with use of X-Ray diffraction (XRD), field emission scanning electron microscopy (FESEM), Fourier transform infrared spectroscopy (FTIR), Raman spectroscopy, and UV-Visible spectrophotometry; structural, optical, and morphological properties of the samples have been evaluated. Using XRD, lattice constants and some related structural parameters were determined. Variation of optical band gap has been calculated too, with aiding absorbance, The XRD data revealed prevailed cubic samarium oxide phase in both samples, even though a sharp diffraction peak of graphene was attended in graphene/samarium oxide sample. SEM, Raman, and FTIR analysis showed the effects of graphene addition on main lattice of samarium oxide. Furthermore, the decrease of optical band gap due to graphene was also notable.

Key words: samarium oxide, graphene, hydrothermal, antimicrobial agent

*Corresponding Author: E-mail: bagherikhatibani@gmail.com

Introduction

Lanthanide oxides or rare earth oxides (REOs) have enticed a lot of consideration since of their chemical, optical, and electronic properties due to their 4f electrons. Rare earth oxides are extendedly employed in different fields such as optical tools, luminescence devices, heterogeneous catalysis, glass industries, fuel cells, biochemical probes, and medical diagnostics. Since the rare earth ions have generically trivalent state, they are abiding compounds. Between rare earth oxides, Sm_2O_3, as a p-type semiconductor, tends to interchange lattice oxygen facilely with air. This is an efficient way to keep stoichiometry of the oxides (Dezfuli et al.,2017; Mansoob Khan & Najihah Matussin, 2023).

It is proven that the shape and size of particles are critical parameters for engineering material features to represent exclusive and attractive optical, magnetic, and electronic properties for hopeful applications in different fields (Busatto & Donega, 2022). During past years, nano-sized materials have been have been extensively reviewed, because of the difference in their properties compared to bulk form (Khan et al., 2019). It is known that rare earth ions nanoparticles materials are greatly photostable with long luminescence lifetimes and slender emission bands (Heiba & Bakr Mohamed, 2020). Shape-controlled samarium oxide nanocrystal is a hopeful topic for the bottom-up assembly of new nanostructure with vast applicability in different area, like as in biochemical sensors, nano-electronics, gas sensors, and solar cells (Mansoob Khan & Najihah Matussin, 2023).

It is believed that rare earth elements and related oxides such as samarium, erbium, yttrium, europium, and cerium face deficiency of electrical conductivity which can be invigorated with synergistic effect by making a composite with graphene based structures (Anitha et al., 2022). Graphene, as an allotrope of carbon, have a single sheet of carbon atoms separated from graphite. Graphene has got much consideration because of its great surface area, significant mechanical, thermal, and optical features (Javaid & Akhyar Farrukh, 2023). Graphene, as a significant member of the carbon family, is a promising material for various applications. It's astonishing physicochemical properties like extraordinary current density, exceptional elasticity, fantastic Young's modulus, brilliant fracture strength, incredible thermal conductivity, high corrosion resistance, fascinating self-lubricating behavior, phenomenal chemical stability, high hydrophobicity, suitable electron mobility, amazing transparency, and standout mechanical strength flexibility are just a few pieces of the capacities of this material. Furthermore, it's supple, slim and two-dimensional nature with great surface area makes it an outstanding framework (Saadat Niavol et al., 2024). Another reason to be interested in this substance is decorating ability of graphene based materials with different nano-materials. The acquired hybrid nano-materials have attractive properties which may be adjusted by changing the loading value, and loaded nano-material on the graphene based sheets (Hu et al., 2016)

Various metal oxides such as SnO_2, Mn_3O_4, ZnO, MnO_2, CeO_2, and RuO_2 have been used for the decoration graphene based compounds. The presence of these compounds hinders the graphene sheets restacking and prevents losing of the surface area. Hence, loading such nano-materials to graphene sheets cause to more access to the surface of the graphene by creating space between the graphene sheets (Dezfuli et al., 2015). Such spaces made among the graphene sheets reduce the internal resistance of the materials.

The samarium oxide/graphene based nanocomposite can be obtained through different technics such as sol–gel, co-precipitation, green synthesis, and hydrothermal method (Mansoob Khan & Najihah Matussin, 2023). Among these methods, the hydrothermal method has a distinct parade. It makes an appropriate connection among the materials used. It is possible to synthesize the desired materials in a different level of temperature, pH, and pressure conditions. Controlling of the nanomaterials morphology can be made by liquid phase or multiphase reactions (Lima et al., 2022).

Among the potential and practical applications of samarium oxide and samarium oxide / graphene, biological application has a special position. Muthulakshmi et al. (Muthulakshm

et al., 2020) studied samarium oxide nano-particles as antibacterial and antioxidant agents. It was used against *Staphylococcus aureus* and *Escherichia coli*. The results represented inhibition zones between 15 and 17 mm and 17 and 22 nm, respectively. Samarium oxide nanoplatelets have been applied as a glucose oxidase biosensor by Leote et al. (Leote et al., 2022). This biosensor was examined for glucose sensing in serum samples with a 90% recovery factor. Graphene doped samarium oxide nanocomposites were used by Javaid et al. (Javaid & Akhyar Farrukh, 2023) to evaluate pathogenic bacterial strains of *Escherichia coli*, *Staphylococcus aureus*, and *Pseudomonas aeruginosa*. No antimicrobial results have been perceived against *Escherichia coli* and no inhibition zone has been created for any nanocomposite suspension. The positive antimicrobial activity was viewed by the samarium oxide/graphene nanocomposite against *Pseudomonas aeruginosa* by spreading a 1.2 and 1.6 cm inhibition zone for 30 and 60 µl suspension of the sample, respectively. For *Staphylococcus aureus*, a 2.5 cm inhibition zone was witnessed for a 60 µl suspension of the sample. Zahmatkesh et al. investigated the effects of samarium oxide nanoparticles on biofilm, virulence factors, and motility of multidrug-resistant *P. aeruginosa*. They showed that samarium oxide nanoparticles (Sm_2O_3NPs) significantly inhibited biofilm formation of *P. aeruginosa* by 49–61%. Additionally, sub- minimum inhibitory concentration (MICs) amounts of Sm_2O_3NPs effectively decreased virulence factors including pyocyanin (33–55%), protease (24–45%), and hemolytic activity (22–41%). Moreover, swarming, swimming, and twitching motility remarkably was reduced after exposure to the NPs.

Alshahrani et al. synthesized silver nanoparticles (Ag-onion), samarium oxide nanoparticles (Sm_2O_3-onion), and silver/samarium oxide core/shell nanoparticles (Ag@Sm_2O_3-onion) by the aqueous onion peel extract (OPE). OPE and NPs were tested for the disinfection of some water microbes. The isolated bacteria from the water sample were *Bacillus subtilis*, and *Escherichia coli*, while the isolated fungi were *Alternaria brassicae*, *Aspergillus flavus, Aspergillus penicillioides, Pythium ultimum, Verticillium dahlia, Fusarium acuminatum, Candida albicans, and Candida parapsilosis*. High levels of antimicrobial activity have been reported for nanoparticles.

In this article, the mesoporous pure samarium oxide and graphene/samarium oxide nanocomposites have been prepared through an effective hydrothermal route. The structural, morphological, and optical features of the prepared samples were evaluated through X-ray diffraction (XRD), field emission scanning electron microscopy (FESEM), Fourier transform infrared (FTIR), Raman spectroscopy, and Uv-visible spectrophotometry.

Experimental

Preparations of the samples

For preparing samarium oxide nano-structure, a specific amount of Sm(NO3)3 · $6H_2O$ has been dissolved in distilled water (12.5 ml). This solution was subjected to magnetic stirring to acquire 0.06M solution. To keep the pH level, ammonia was inserted drop wise. 12.5 ml cetyl trimethyl ammonium bromide (CTAB) was also added to this collection. After that, it was moved to autoclave (100 ml), sealed and kept at 120 °C for 3 h. Through centrifugation, the acquired precipitate was separated, washed with distilled water and ethanol several times and annealed at 600 °C for 1 h. For obtaining graphene/samarium oxide nano-composite, 80 mg of prepared samarium oxide was poured into 50 ml of deionized water and stirred for 30 minutes and ultrasonicated for 30 minutes. Then 30 mg of graphene was added to it and this procedure continued with 1h stirring and 30 min. being in ultrasonic chamber. The final product was moved to autoclave (100 ml), sealed and kept at 90 °C for 3 h. In the next steps, centrifugation, washing with distilled water and ethanol, and drying at 70 °C for 24 h were applied to the material obtained.

Methods and analysis

The X-ray diffraction (XRD) analyzer (Philips PW1730) with Cu_Kα radiationλ=0.154060 nm) and Fourier transform infrared (FTIR) spectrometer (Tensor 27) were used to detect crystal and bonding structure of the as-prepared samples,

respectively. The morphologies of the powder samples were characterized by field-emission scanning electron microscopy (FESEM, Tescan Miraii) equipped with an energy dispersive X-ray (EDX). Raman spectroscopy analyses were conducted with a micro-Raman apparatus with a 473 nm wavelength laser. Optical absorbance for samples was measured with a Varian Cary100 UV/visible spectrophotometer.

Results and discussion

XRD results

The XRD patterns of the two samples have been appeared in Fig. 1, and the Miller indices were indexed too. The JCPDS card no.: 43-1029 represents the most compatibility with the XRD data. The crystal planes (211), (222), (400), (332), (134), (440), and (622), in the XRD graph of pristine Sm_2O_3 sample could be referred to cubic samarium oxide structure (Anitha et al., 2022). The polycrystalline nature of the sample is obvious. The sharp diffraction peak at 2θ values of 26.8° can be attributed to the (002) plane of graphene according to the JCPDS card no.: 08-0415.

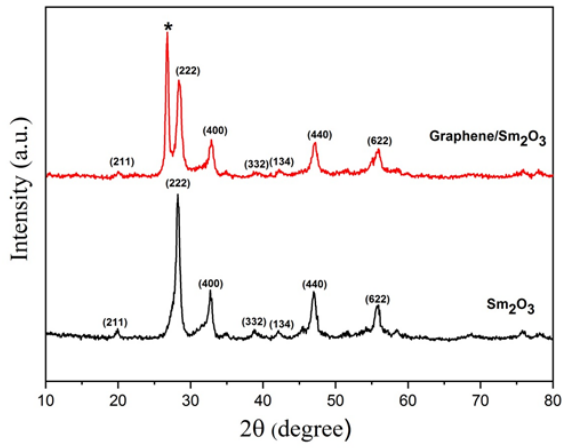

Fig. 1 XRD patterns of pure and graphene added Sm_2O_3 samples with the relevant reflection planes

The lattice parameters have been evaluated and tabulated in Table 1. The calculated values of the certain (222) plane are placed close to the related standard values to make it easier to compare them. The resulted lattice parameters have been altered due to the addition of graphene that may be ascribed to Vegard's law. Furthermore, the surface energy can be influenced by addition of graphene. The grains with lower surface energy may be transferred, and the movement of atoms to the positions with lower surface energies facilitates these variations (KHADEM CHARVADEH et al., 2022). Reflection peaks are slightly shifted to the higher diffraction angles. It may be justified by Bragg's law; the increment of diffraction angle is equal to the reduction of d-spacing and lattice parameters decrease.

By using the XRD data, some parameters of the samarium oxide structure have been evaluated. The crystallite size, dislocation density, specific surface area, and stacking fault of the sample were estimated through:

$$D = \frac{0.9\lambda}{\beta \cos\theta}$$

$$\delta = \frac{1}{D^2}$$

$$S = \frac{6}{D \times \rho}$$

$$SF = \frac{2\pi^2}{45(3\tan\theta)^{\frac{1}{2}}}\beta$$

Where λ is the X-ray wavelength, β is the angular line width of half maximum intensity, θ is the Bragg's angle and ρ is the density respectively.

It is obvious that the crystallite size decreased for graphene added sample (from about 55 nm to about 23 nm). Other structural parameters show higher values comparatively because they are inversely dependent on the crystallite size value.

The FWHM has a decisive role, since the change of the FWHM changes all related values such as specific surface area, dislocation density, and stacking fault of the samples. Several factors, such as the contraction and expansion of bond length, bond angle, twisting and twinning of crystal structure, and interstitial defects inside the lattice system, can influence the structural parameters.

Table 1 The calculated and standard values of the lattice parameters for the main reflection peak (i.e., (222))

Sample	Miller indices	d (Å)		a (Å)		Volume of unit cell $(Å)^3$	
		Cal.	Sta.	Cal.	Sta.	Cal.	Sta.
Sm_2O_3	222	3.1675	3.1540	10.9725	10.9270	1321.06	1304.68
Graphene/Sm_2O_3	222	3.1571	3.1540	10.9365	10.9270	1308.09	1304.68

Table 2 Some physical properties of pure and graphene added samarium oxide samples related to their structures

Miller indices	FWHM	$D(nm)$	$S \times 10^3(\frac{m^2}{Kg})$	$\delta \times 10^{-5}(nm^{-2})$	stacking fault (SF) $\times 10^{-6}$
222	0.1476	54.55	18.15	33.6	1302
222	0.3444	23.38	42.36	183	3033

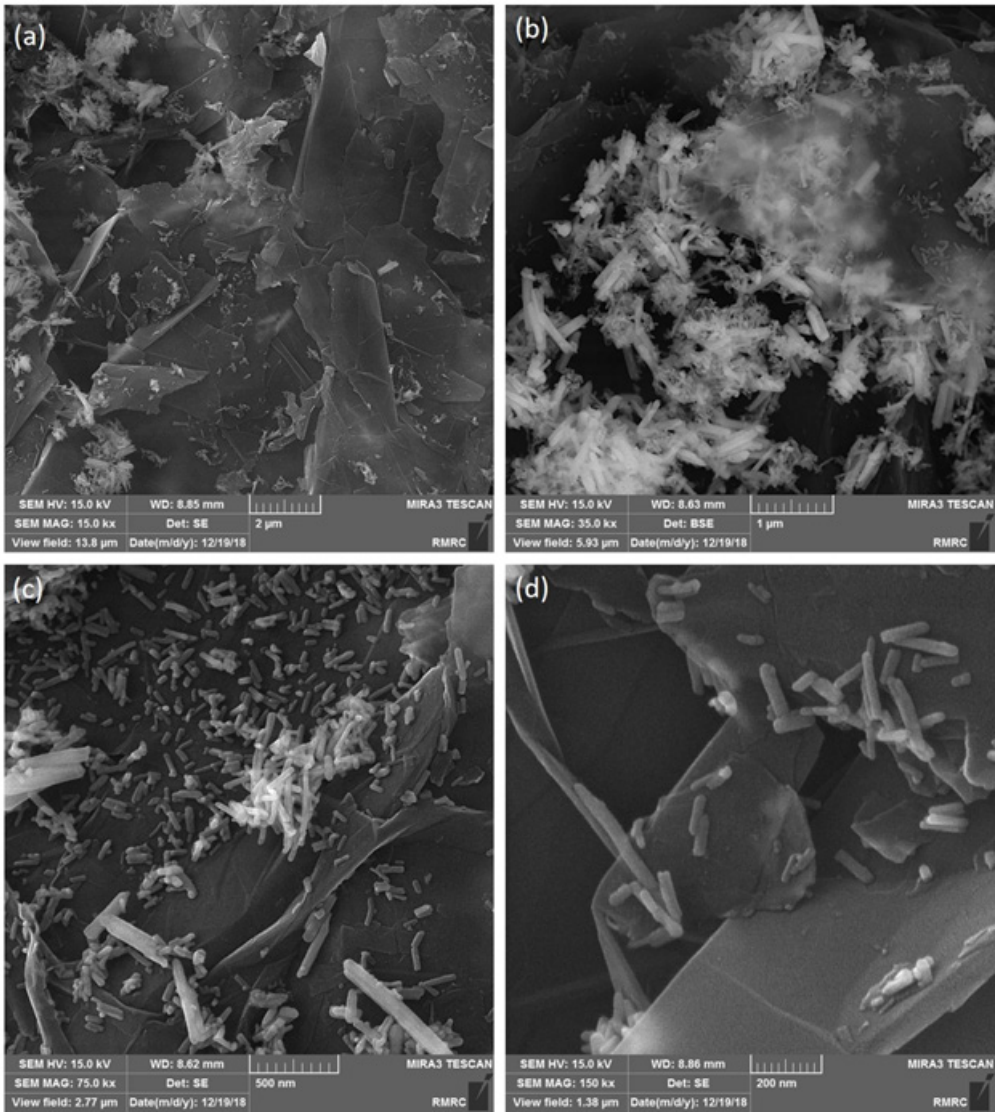

Fig 2. FESEM images of Sm_2O_3 nanorods decorated on Graphene nanoplates in different scales

Biotechnological Journal of Environmental Microorganisms (BJEM)

Biotechnological Journal of Environmental Microorganisms(BJEM) 2(5) 2023 244-252

Fig. 2 (a-d) represents micrographs of Sm_2O_3 nanorods and samarium oxide decorated on graphene nanoplates in different scales. The results clearly show the most horizontally grown samarium oxide nanorods. High magnification SEM images of the nanorods obtained are seen in Fig. 2 b. It appears that the nanorods structure is the only one present. As regard the nanorods size, calculations indicate a mean length of about 400 nm and a mean diameter of about 80 nm. An almost irregular distribution of samarium nanoroads can be observed in the graphen-Sm_2O_3 nanocomposite. This may be a good reason for connection between the graphene nanoplates and samarium nanoroads (Fig. 2 c,d). Moreover, based on Fig. 2c and 2d, the nanorods of samarium oxide are in the range 150 to 200 nm. It is obvious that Sm_2O_3 nanorods are furled by the graphene sheets which prove the establishment of a sandwich-like nanocomposites structure due to the placement of the Sm_2O_3 nanorods between the inter-layer of graphene sheets. This can prohibit the Sm_2O_3 nanorods agglomeration along with avoiding the stacking of graphene sheets and thus leading to maintain their appropriate surface area.

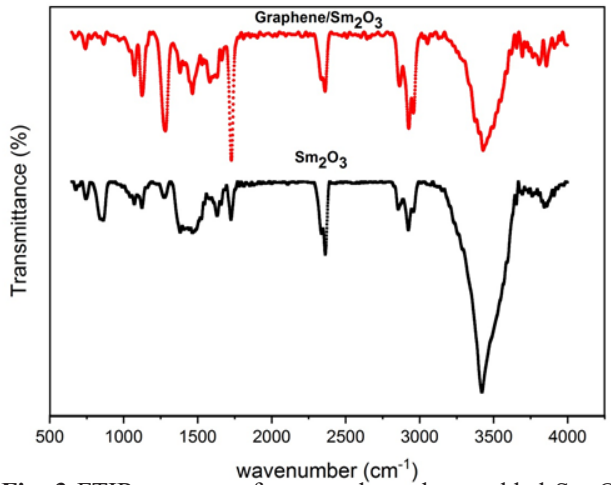

Fig. 3 FTIR patterns of pure and graphene added Sm_2O_3 samples

Fig. 3 shows the FTIR spectra of pristine Sm_2O_3 and graphene/Sm_2O_3 samples. The defined broad band at around of 3425 cm^{-1} belongs to the hydroxyl group (i.e., O–H stretching vibrations) which may relate to the attendance of H_2O on the surface of the samples. The absorption peak around 1630 $cm^{-1}$is due to the presence of CO2 molecule. Of course, the peak situated at around 2360 $cm^{-1}$is due to CO2 in the air. They represent defect states within the main structure. The asymmetric C–H stretching verified through absorption bands presented at 2850 and 2920 cm^{-1}(Saadat Niavol et al., 2022) The C-C vibrations around 1580 cm^{-1}confirmed the attendance of graphene in the graphene added Sm_2O_3 sample (Boukhoubza et al., 2019). In addition, the peak around 1520 cm^{-1}can be ascribed to the stretching vibrations of the OH groups (Saadat Niavol et al., 2022). The absorption peak at 675, 745, and 860 cm^{-1}may be referred to symmetric and asymmetric Sm–O vibration in the samarium oxide structure (Dezfuli et al., 2017). The basic functional group of graphene is located at around 1125 $cm^{-1}$and can be imputed to stretching vibration of C–OH (Saadat Niavol et al., 2022).

Raman analysis is a valuable technique to study the defects and doping features inside a specific structure. This technique can also exhibit small amounts of the defect densities. The Raman data of Sm_2O_3-based samples have been saved between 0 cm^{-1} to 4000 cm^{-1}, as shown in Fig. 4. Two characteristic peaks in 1400 cm^{-1} and 1500 cm^{-1} are attributed to C-C stretching and C-H bending modes. These are known as organic vibrations peaks (Beigli et al., 2023). The observed lines at about 340 cm^{-1} and 450 cm^{-1} can be referred to Sm_2O_3 structure (Rasouli Jamnani et al., 2019). Three peaks at 1360 cm^{-1}, 1580 cm^{-1}, and 2700 cm^{-1}can be ascribed to the D-peak, the G-peak, and the 2D peak, respectively (Fesenko et al., 2015). Some typical parameters such as localized defects, solvents, and doping can change the place of vibration peaks. This can double the importance of the Raman analysis in determining these displacements. The G-peak is attributed to the C-C bond stretching. The D-peak is referred to impurity and disorder in the graphene sample. The 2D peak is a typical peak for graphite based samples. It is interesting that the characteristics of this peak like the location, the intensity, and the width can represent layers amount. The intensity of the D peak in comparison with G and 2D indicates that there is not much disorder in the graphene/Sm_2O_3 sample.

The structural regularity of carbon nanomate-

Biotechnological Journal of Environmental Microorganisms (BJEM)

Biotechnological Journal of Environmental Microorganisms(BJEM) 2(5) 2023 244-252

rials is usually expressed by the intensity ratio of the D band versus the G band (ID/IG). The lower the ID/IG value, the more regular the carbon nanomaterials (Zhang et al., 2019). This ratio provides valuable information about the structural disorder and defects in the carbon-based material. A higher ratio indicates a higher level of structural disorder and defects, while a lower ratio indicates fewer defects and a more ordered structure. The ID/IG value of graphene added Sm_2O_3 is 0.62. The I2D/IG was also estimated and equals to 2.1.

The optical properties of both nanocomposites were studied through UV-visible spectroscopy and represented in Fig. 5. Optical absorbance data of the samples were recorded in the range of 200–1100 nm. Comparing the two graphs shows that the presence of graphene has affected the absorbance of samarium oxide and created a clear absorption edge at 270 nm. After the wavelength of 500 nm, the amount of optical absorption has decreased slightly with the presence of graphene.

Multiple parameters such as packing density, porosity, and surface properties can influence the absorbance. Some morphological features such as grain size and grain boundaries are also effective. It is known that the lower grain size and bigger grain boundaries cause to greater absorbance (Khatibani, 2019).

The optical energy gap can be obtained via absorbance data. It is generally dependent on the

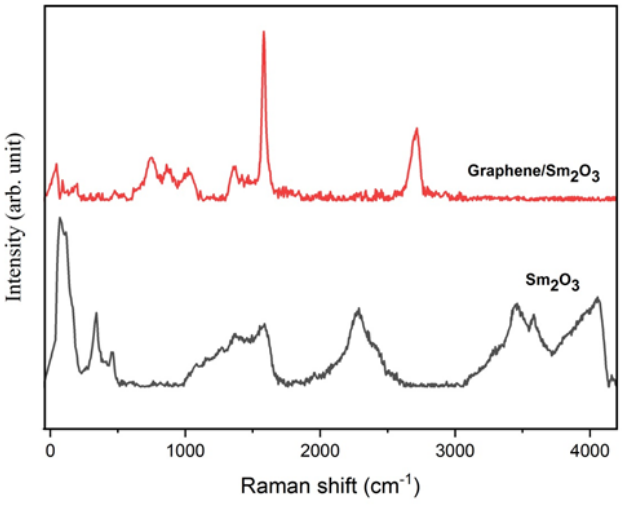

Fig. 4 Raman spectra of samarium oxide based samples at room temperature

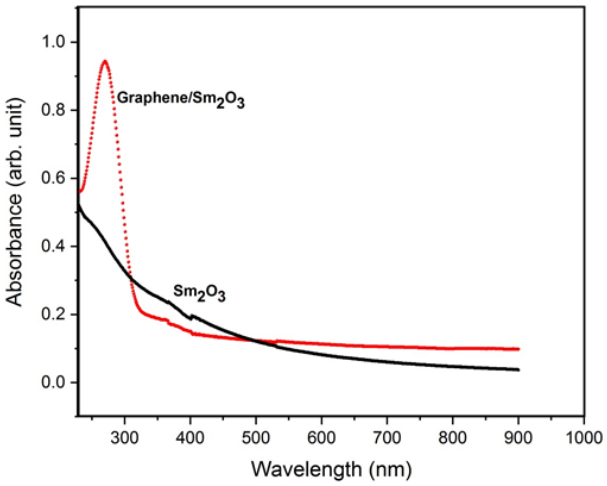

Fig. 5 Optical absorbance of samarium oxide based samples at room temperature

structural property of the samples. The absorption and the photon energy are related parameters which are expressed as follows:

$$(\alpha h\nu)^{1/N} = A(h\nu - E_g)$$

where α means the absorption coefficient , A is a constant, E_g denotes the optical band gap, and the exponent N relates to the type of transition. It can be $\frac{1}{2},2,\frac{3}{2},3$ which indicates the allowed direct, allowed indirect, forbidden direct and the forbidden indirect, respectively (Bagheri Khatibani et al., 2013). Absorption coefficient can be evaluated by different methods, one of them is:

$$\alpha = 2.303\frac{A}{t}$$

The evaluation of optical band gap is obtained via extrapolation of the linear part of the absorption curve until they cut the horizontal axis. Based on Fig. 6, the band gap of the allowed direct transition for two samples is 4.95 eV, and 4.58 eV, respectively. This reduction is in agreement with Javaid et al. (Javaid & Akhyar Farrukh, 2023).

It is rightly observed that the addition of graphene decreases the band gap energy. The decrease in the band gap in nanocomposite samples as compared to pure Sm_2O_3 can be attributed to the variation in the crystallite size and due to the existence of an interaction between Sm-O-C atoms in graphene added Sm_2O_3 nanocompos-

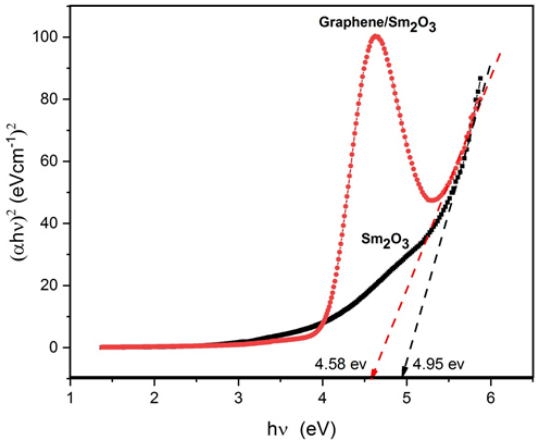

Fig. 6 Optical bandgap of pure and graphene added Sm_2O_3 samples

ite. Thus, it can be predicted that pure samarium oxide while synergizing with graphene may enhance the efficiency to use it to study photocatalytic activity or to design devices to capture visible light response for different purposes.

It is known that the band gap energy is influenced by multiple factors such as grain size, contraction or extension of the lattice, lattice strain, quantum size effect, quantum confinement, structural or thermal disorder, and native defects (Khatibani, 2019).

Although a lot of research has been done or is being done on antimicrobial agents, the combination of graphene-samarium oxide has not been studied much. Considering the wide application of these two substances, it seems that it can be used as an effective antimicrobial agent.

Conclusion

Pure and graphene added samarium oxide nano-structures have been prepared by simple hydrothermal route. After going through the preparation steps, their optical, structural, and morphological features have been studied and compared. XRD, FESEM, FTIR, Raman, and absorbance data were informative and distinctive. From morphological view, a wide irregular distribution of samarium nanoroads is observed in the graphen-Sm_2O_3 nanocomposite. This verified the good connection between the graphene nanoplates and samarium nanoroads. Particular absorption bands (i.e. at 675 , 745 , and 860) in FTIR are referred to Sm–O vibration in the samarium oxide lattice structure. In Raman analyze, the observed lines at about 340 cm^{-1}, and 450 cm^{-1} can be ascribed to Sm_2O_3 structure. The intensity of the D peak in comparison with G and 2D indicates that there is not much disorder in the graphene/Sm_2O_3 sample. The calculations showed that the band gap energy decreased after addition of graphene. The band gap values of the allowed direct transition for two samples are 4.95 eV, and 4.58 eV, respectively.

References

Alshahrani A. A., Alqarni L. S. , Alghamdi M. D., Nasser F. Alotaibi N. F., Moustafa S. M. N., Amr M. Nassar A.M. (2024). Phytosynthesis via wasted onion peel extract of samarium oxide/ silver core/shell nanoparticles for excellent inhibition of microbes. Heliyon, 10, e24815.

Anitha M., Velvizhi K., Mohamed Ismail M., Shanmugam M., Arivanandhan M., Anandan P. (2022). Enhanced electrochemical performance of rGO: Sm_2O_3 nanocomposite synthesized by hydrothermal assisted simple solution technique. Journal of Materials Science: Materials in Electronics, 33, 27076–27091.

Bagheri Khatibani A., Rozati S. M., Hallaj Z. A. (2013). Synthesis and characterization of nanostructure CdO:Zn thin films deposited by spray pyrolysis technique: Molarity and heat treatment effects, Materials Science in Semiconductor Processing, 16(3), 980-986.

Beigli H., Shaddoust M., Ahmadi M.H., Bagheri Khatibani A. (2023) Effect of low and relatively long-term gamma irradiation on physical properties of ZnO and ZnO: Co thin films, Journal of Sol-Gel Science and Technology, 108, 798–808.

Busatto S. & Donega C. D. M. (2022). Magic-Size Semiconductor Nanostructures: Where Does the Magic Come from?, ACS Materials Au, 2(3), 237–249

Boukhoubza I., Khenfouch M., Achehboune M., Moses Mothudi B., Zorkani I., Jorio A. (2019). Graphene oxide/ZnO nanorods/graphene oxide sandwich structure: The origins and mechanisms of photoluminescence, Journal of Alloys and Compounds, 797, 1320-1326.

De Lima B. S., Komorizono A. A., Ndiaye A. L., Bernardi M. I. B., Brunet J., Mastelaro V. R. (2022). Tunning the Gas Sensing Properties of rGO with In_2O_3 Nanoparticles. Surfaces, 5, 127–142.

Dezfuli A.S., Ganjali M.R., Naderi H.R., Norouzi P. (2015). A high performance supercapacitor based on a ceria/graphene nanocomposite synthesized by

a facile sonochemical method. RSC Advances, 5, 46050-46058.

Fesenko O., Dovbeshko G., Dementjev A., Karpicz R., Kaplas T., Svirko Y. (2015). Graphene-enhanced Raman spectroscopy of thymine adsorbed on single-layer graphene, Nanoscale Research Letters, 10, 163

Heiba Z. K. & Bakr Mohamed M. (2020). Effect of Gamma radiation on structural and opticalparameters of Sm_2O_3:Mn/PVA nanocomposite film, Optical and Quantum Electronics, 52, 99.

Hu N., Zhang L., Yang C., Zhao J., Yang Z., Wei H., Liao H., Feng Z., Fisher A., Zhang Y. (2016). Three dimensional skeleton networks of graphene wrapped polyaniline nanofibers: an excellent structure for high-performance flexible solid-state supercapacitors, scientific reports, 6, 19777.

Javaid A. & Akhyar Farrukh M. (2023). Comparison of photocatalytic and antibacterial activities of allotropes of graphene doped Sm_2O_3 nanocomposites: Optical, thermal, and structural studies. Journal of the Chinese Chemical Society, 70, 32–45.

KHADEM CHARVADEH S., NEJATINIA S., BAGHERI KHATIBANI A., AHMADI M.H. (2022). Growth, characterization and investigation of gas-sensing performance of graphene and copper-doped zinc oxide prepared by sol–gel method, 45, 61.

Khan I, Saeed K, Khan I. (2019), Nanoparticles: Properties, applications and toxicities, Arabian Journal of Chemistry, 12(7), 908-931.

Khatibani A.B. (2019). Characterization and ethanol sensing performance of sol-gel derived pure and doped zinc oxide thin films. Journal of Electronic Materials, 48, 3784.

Leote R. J. B., Matei E., Apostol N. G., Enculescu M., Enculescu I. , Diculescu V. C. (2022). Monodispersed Nanoplatelets of Samarium Oxides for Biosensing Applications in Biological Fluids. Electrochimica Acta, 402, 139532.

Mansoob Khan M., Najihah Matussin S. (2023). Sm_2O_3 and Sm_2O_3-based nanostructures for photocatalysis, sensors, CO conversion, and biological applications. Catalysis Science & Technology, 13, 2274.

Muthulakshmi V., Balaji M., Sundrarajan M. (2020). Biomedical Applications of Ionic Liquid Mediated Samarium Oxide Nanoparticles by *Andrographis Paniculata* Leaves Extract. Materials Chemistry and Physics, 242, 122483,

Rasouli Jamnani S., Milani Moghaddam H., Leonardi S.G., Donato N., Neri G. (2019). Synthesis and characterization of Sm_2O_3 nanorods for application as a novel CO gas sensor. Applied Surface Science, 487, 793-800,

Saadat Niavol S., Milani Moghaddam H., Bagheri Khatibani A., Hashemi Karouei S.F., Hermerschmidt F., Ligorio G., List-Kratochvil E. J. W. (2022). Enhancing both methylene blue photocatalytic degradation and ethanol sensing performances of ZnO/rGO nanocomposite through the variation of GO amount, Applied Physics A, 128, 733.

Saadat Niavol S., Bagheri Khatibani A., Milani Moghaddam H., Gao G. (2024), ZnO quantum dots decorated on graphene oxide and graphene nanoplatelets: Comparison the structure and sensing properties, Inorganic Chemistry Communications, 160, 111957.

Shiralizadeh Dezfuli A., Ganjali M. R., Naderi H. R. (2017). Anchoring Samarium Oxide Nanoparticles on Reduced Graphene Oxide for High-Performance Supercapacitor. Applied Surface Science, 402, 245-253.

Zahmatkesh H., Mirpour M., Zamani H., Rasti B., Asadi Rahmani F., Padasht N., (2022). Effect of samarium oxide nanoparticles on virulence factors and motility of multi-drug resistant *Pseudomonas aeruginosa*, World Journal of Microbiology and Biotechnology 38, 209.

Zhang J., Zhang Z., Jiao Y., Yang H., Li Y., Zhang J., Gao P. (2019). The graphene/lanthanum oxide nanocomposites as electrode materials of supercapacitors, Journal of Power Sources, 419,99-105.